Supplementary Information for: Korean Lunar Navigation Constellation with Stability-Filtered Optimisation

Seungsoo Yoo[1], **Gyu-In Jee**[1], **and Sun Yong Kim**[1,*]

[1]Konkuk University, Department of Electrical and Electronics Engineering, Seoul, 05029, Republic of Korea
[*]kimsy@konkuk.ac.kr

ABSTRACT

This Supplementary Information accompanies the manuscript “Korean Lunar Navigation Constellation with Stability-Filtered Optimisation” and provides additional figures and tables that complement the main text. The Supplementary Figures (S1–S9) include spatial heatmaps of the number of visible satellites and geometric dilution of precision, near-side latitude profiles, the three-dimensional baseline+KLNS constellation geometry, KLNS ground tracks, Keplerian-versus-perturbed divergence maps, elevation-mask sensitivity, weight sensitivity, and scalability analysis. The Supplementary Tables (S1–S8) include the per-stage incremental performance, long-term Keplerian-versus-perturbed comparison, frozen-orbit element ranges, multi-threshold GDOP availability, elevation-mask sensitivity, site-specific PNT performance, link budget, and the stability-filter outcome counts. Items are numbered in the order they appear in the corresponding subsection of the main manuscript.

Supplementary Figures

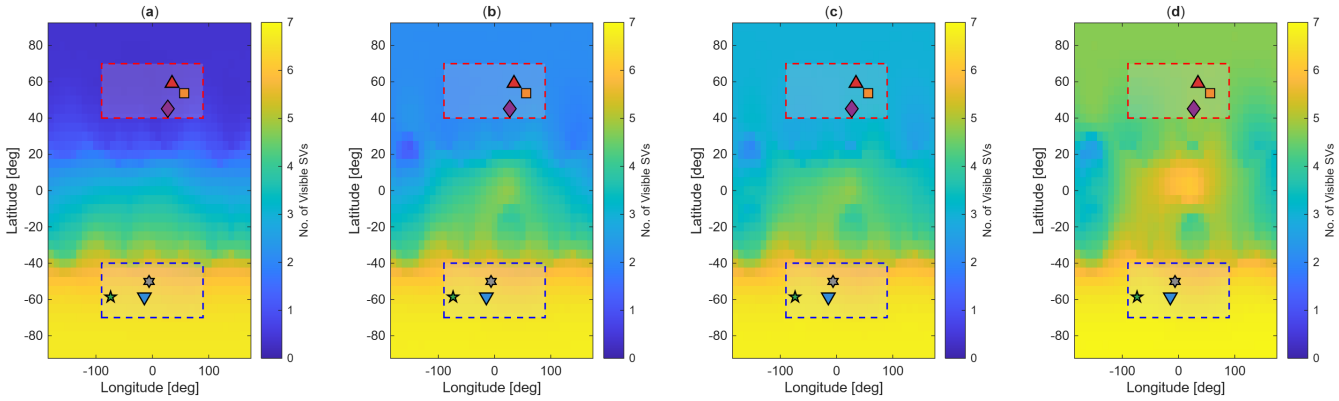

Figure S1. NVS heatmaps at four deployment stages: (**a**) Base(8); (**b**) +2(10); (**c**) +3(11); (**d**) +5(13). KASA candidate landing sites are marked with symbols.

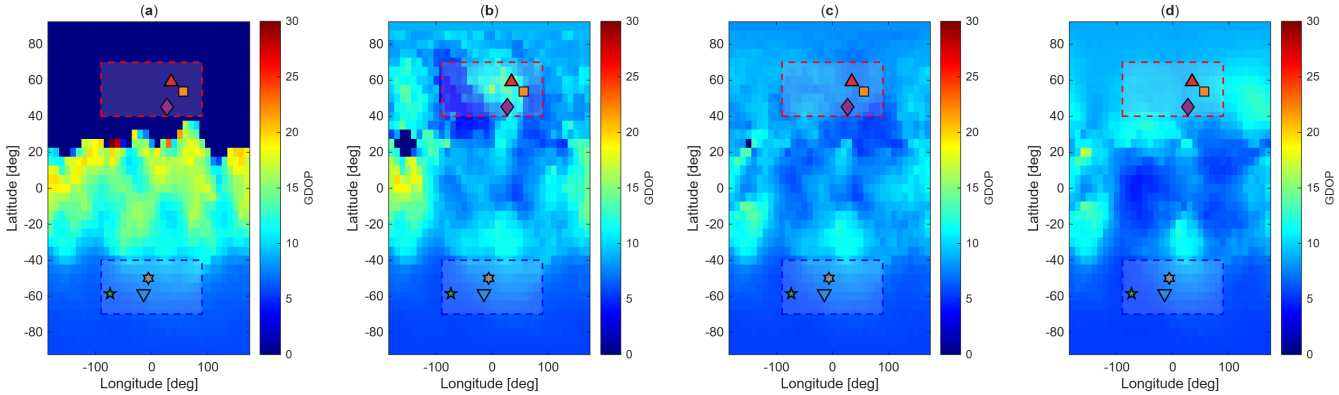

Figure S2. GDOP heatmaps at four deployment stages: (**a**) Base(8); (**b**) +2(10); (**c**) +3(11); (**d**) +5(13). Values below 15 (yellow–green) indicate good positioning geometry; the final stage (+5) shows almost the entire near-side at GDOP$\leq$15 except a residual band near 30°N.

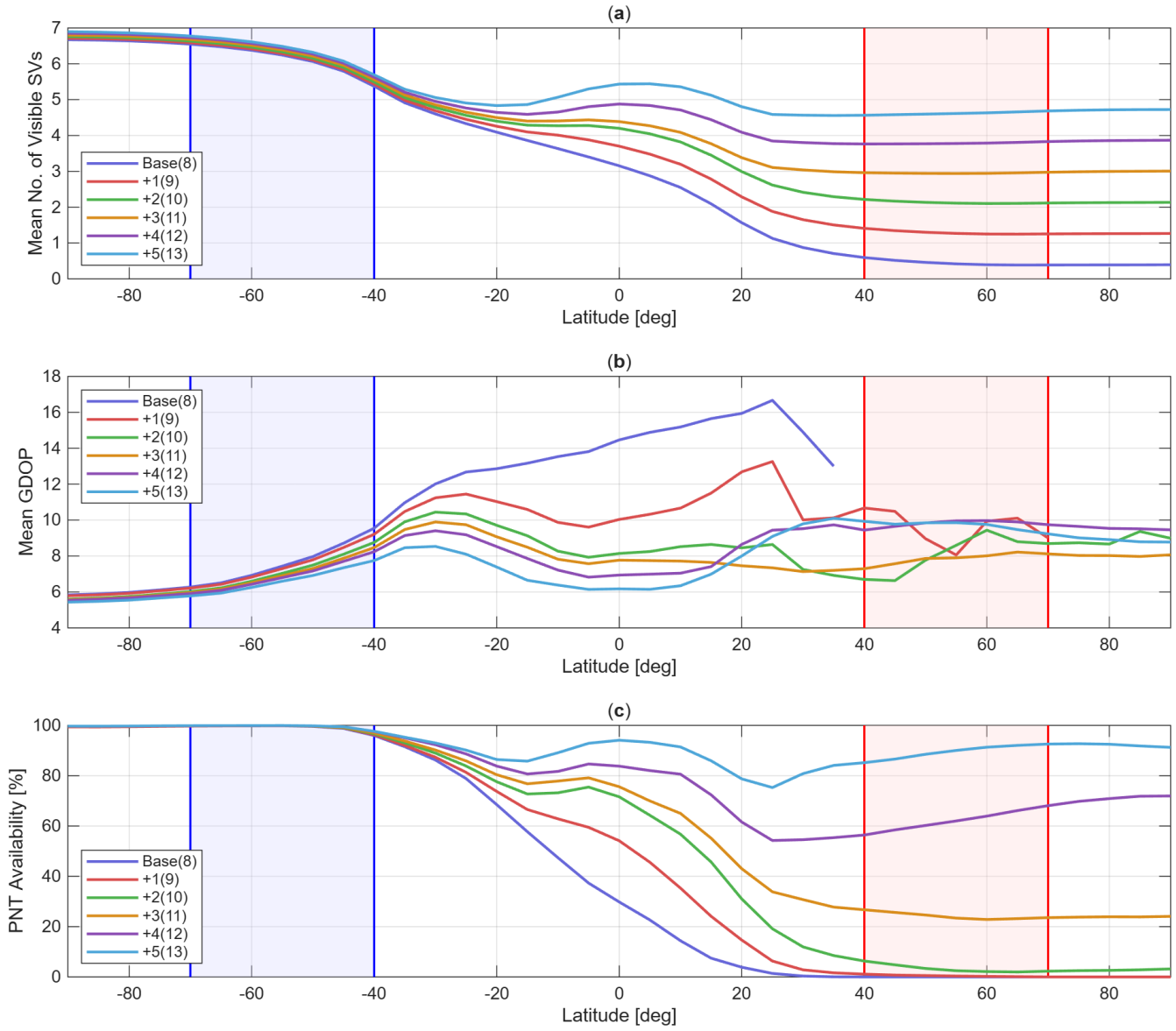

Figure S3. Near-side longitude-averaged latitude profiles at every deployment stage: (**a**) mean NVS; (**b**) mean GDOP; (**c**) PNT availability. The N-ROI (40°–70°N) is shaded in red and the S-ROI (40°–70°S) is shaded in blue. In panel (**b**), curves terminate where the longitude-averaged GDOP becomes undefined because more than half of the longitude cells in that latitude bin have NVS<4 at most epochs: this occurs above ∼28°N for Base(8) and above ∼35°N for +1(9), highlighting precisely the mid-latitude geometry deficit that the KLNS augmentation is designed to close.

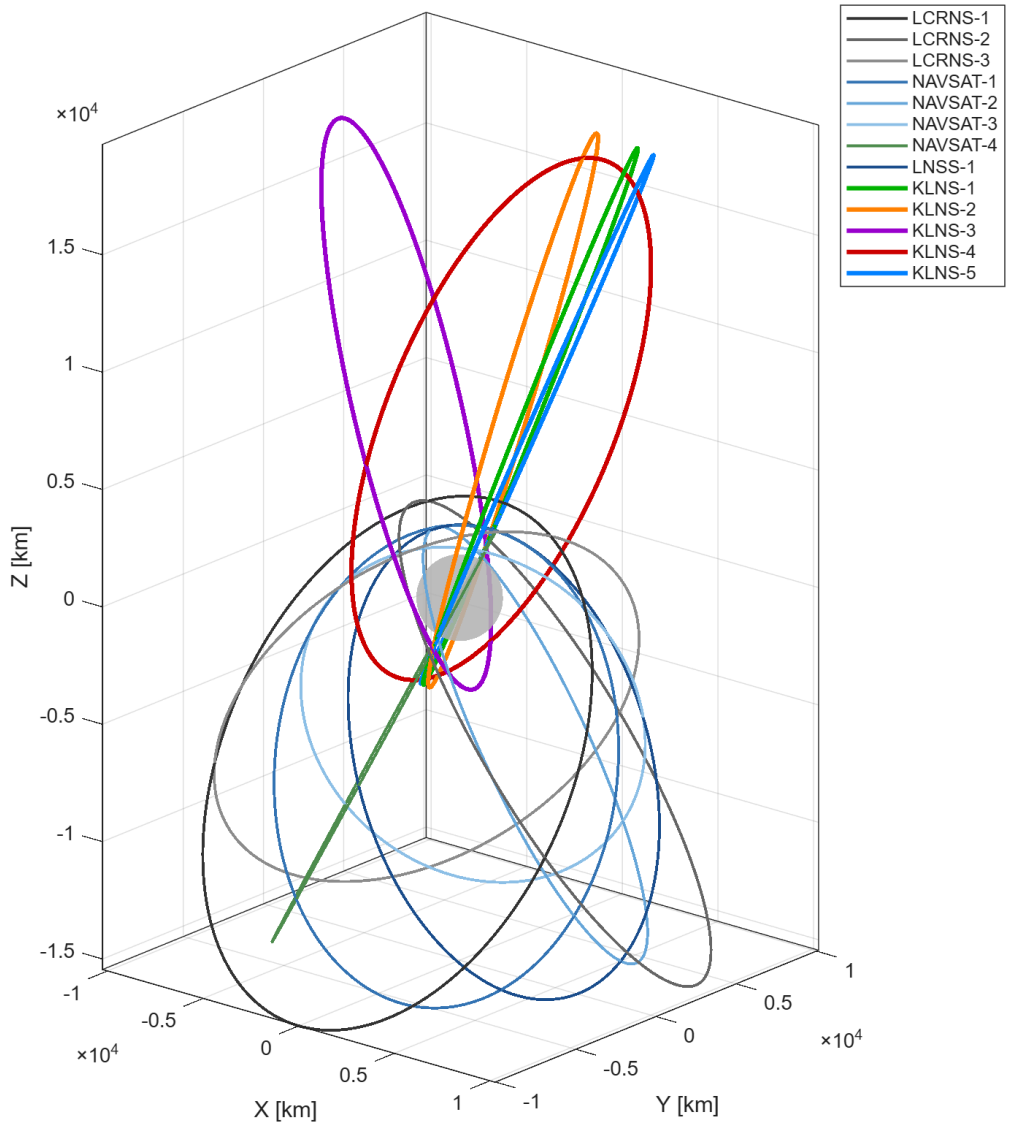

Figure S4. Three-dimensional orbit plot of the baseline (8) + KLNS (5) constellation over one orbital period. The five KLNS orbits (high-altitude ELFOs with $\omega = 270^\circ$) loop over the northern hemisphere, complementing the southern-hemisphere apoapsis of the baseline.

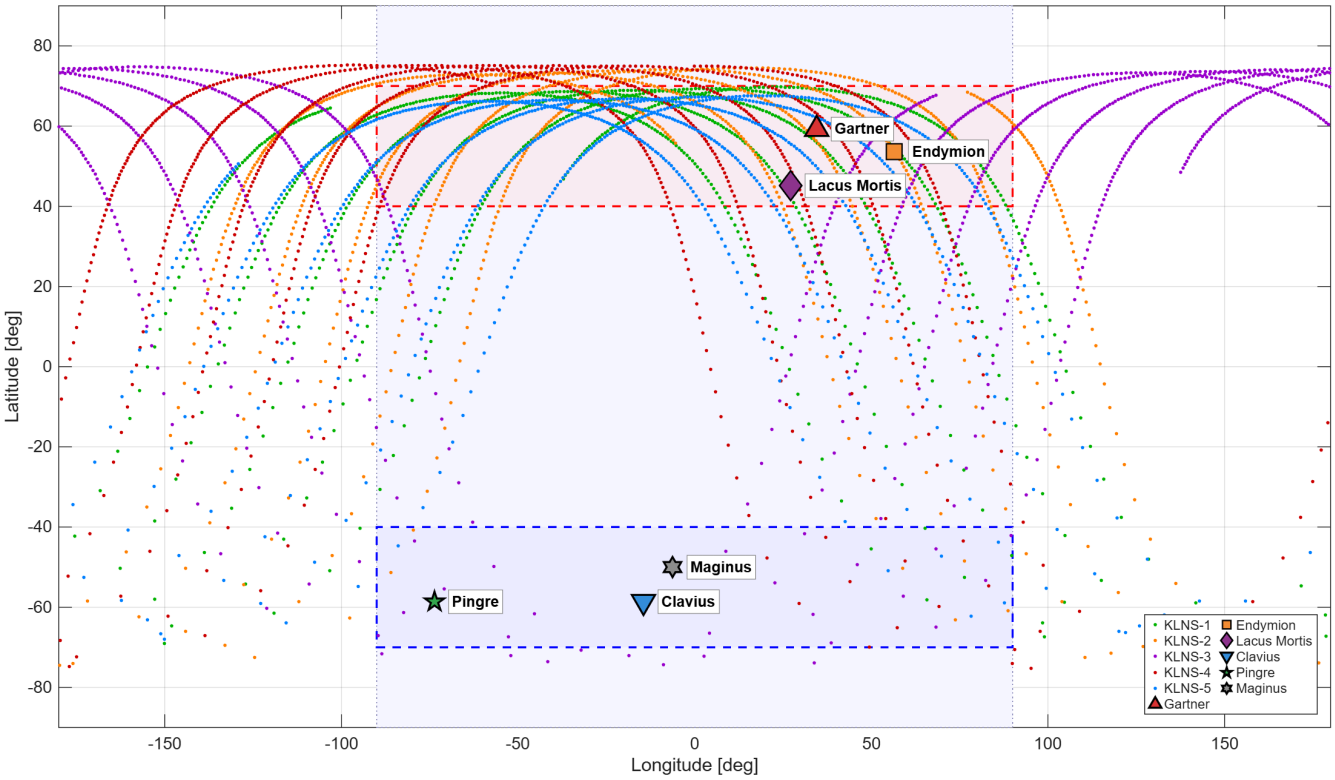

Figure S5. KLNS ground tracks (168 h) with KASA candidate landing sites annotated. The N-ROI (40°–70°N) and S-ROI (40°–70°S) are shaded; KLNS dwell over the N-ROI is clearly visible from the dense track concentration in the upper near-side band.

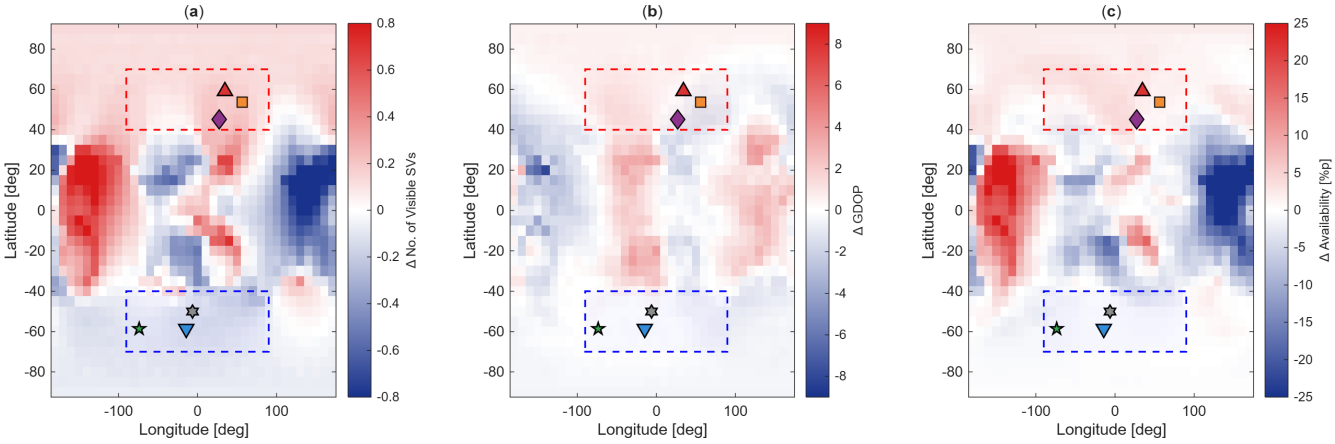

Figure S6. Keplerian vs. perturbed divergence at 720 h: (**a**) ΔNVS; (**b**) ΔGDOP; (**c**) ΔAvail. The differences are spatially patchy but bounded: $|\Delta\text{NVS}| \leq 0.8$, $|\Delta\text{GDOP}| \leq 9$, $|\Delta\text{Avail}| \leq 25$ percentage points at any single grid cell.

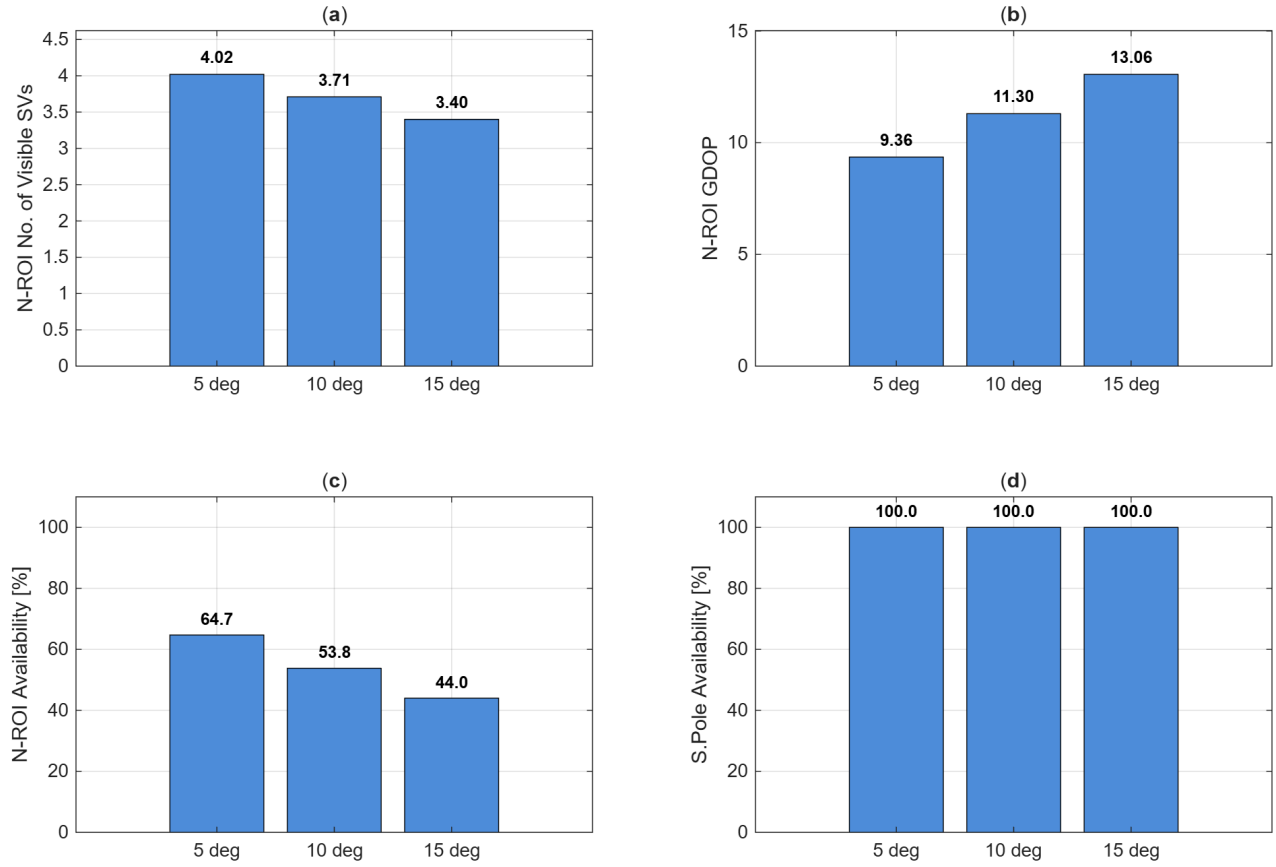

Figure S7. Elevation mask sensitivity for the 13-satellite constellation: (**a**) N-ROI mean NVS; (**b**) N-ROI mean GDOP; (**c**) N-ROI PNT availability; (**d**) South Pole availability. The N-ROI availability degrades gracefully from 64.7% at 5° to 44.0% at 15°; the South Pole availability remains 100% throughout.

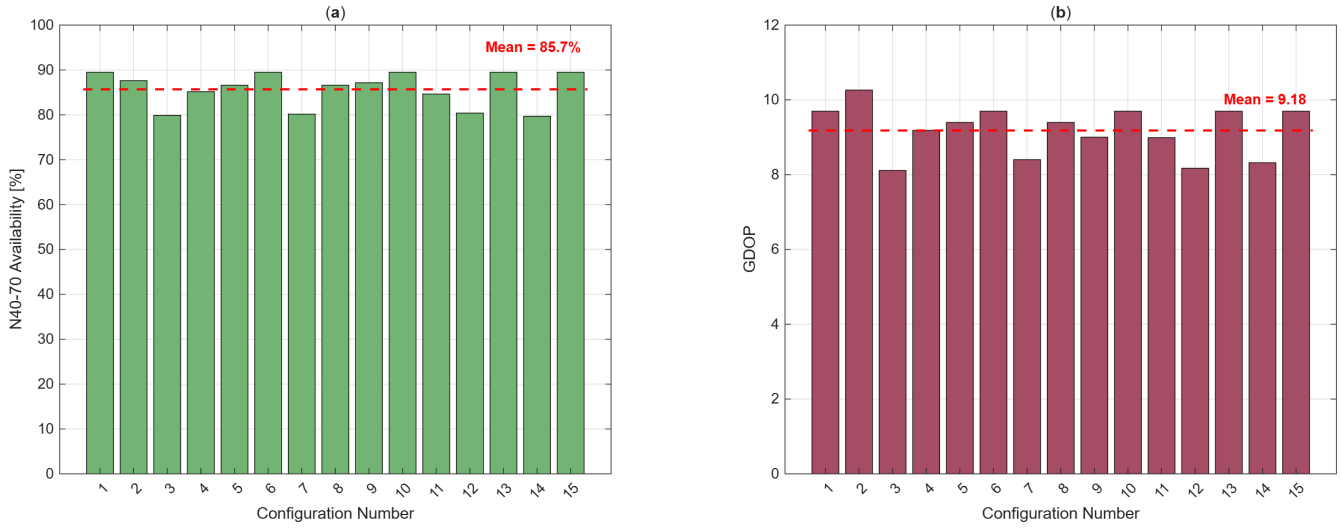

Figure S8. Weight sensitivity across 15 weight configurations: (**a**) N40–70 availability; (**b**) N40–70 GDOP. All 15 configurations exceed 79% availability, with the spread (9.8%p) narrower than observed in unfiltered formulations.

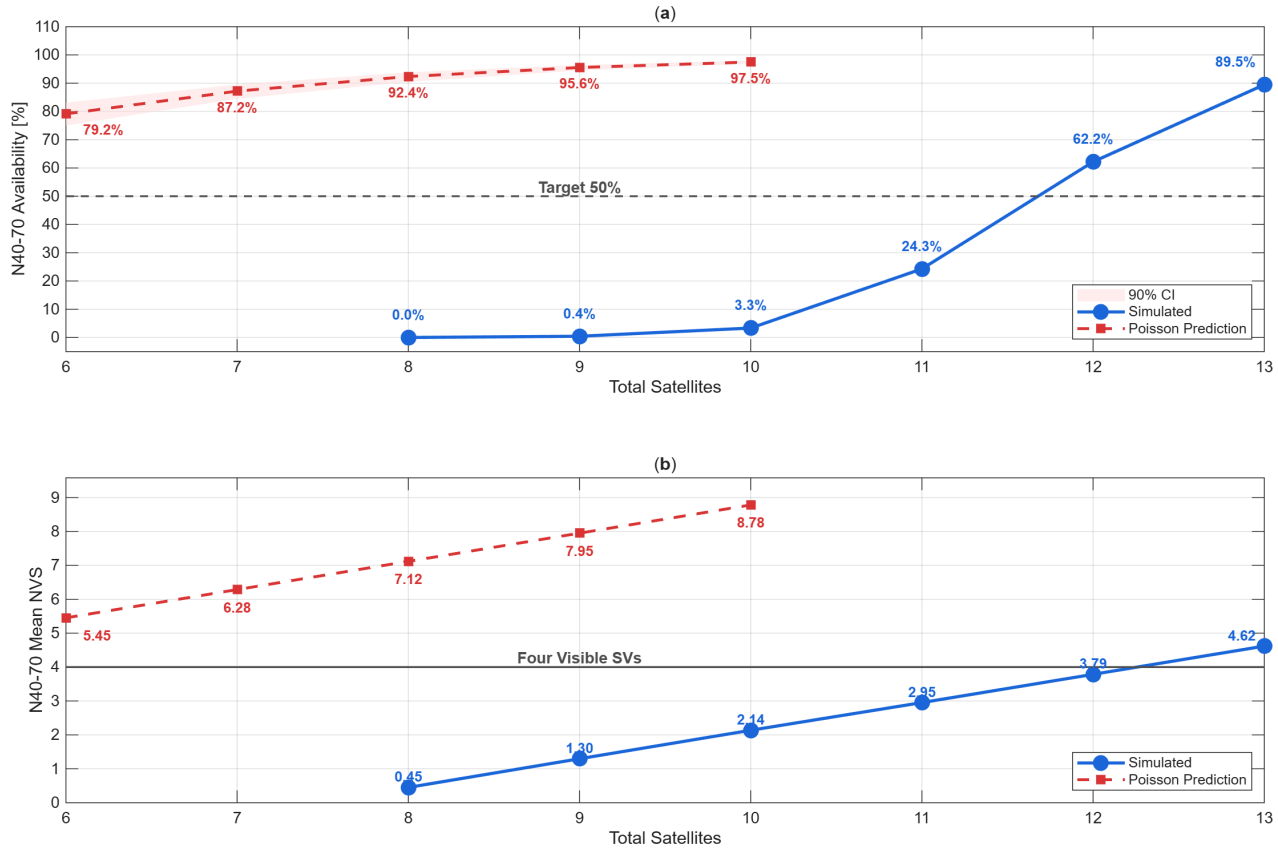

Figure S9. Scalability analysis vs. total satellite count, with Poisson prediction and 90% confidence interval: (**a**) PNT availability; (**b**) mean NVS. The simulated points (8–13 satellites) follow a sigmoidal growth, and the Poisson model projects ∼95% availability at 14–15 satellites.

Supplementary Tables

Table S1. Incremental PNT performance (168 h, perturbed model, $\varepsilon_{\min} = 5^\circ$).

Metric	Base(8)	+1(9)	+2(10)	+3(11)	+4(12)	+5(13)
N-ROI NVS	0.45	1.30	2.14	2.95	3.79	4.62
N-ROI GDOP	—	9.91	8.09	7.85	9.79	9.70
N-ROI Avail [%]	0.00	0.40	3.30	24.30	62.20	89.50
S-ROI NVS	6.13	6.21	6.30	6.42	6.52	6.62
S-ROI GDOP	7.63	7.46	7.21	6.93	6.74	6.51
S-ROI Avail [%]	99.10	99.20	99.30	99.40	99.50	99.50
S. Pole Avail [%]	99.4	99.4	99.7	99.7	99.7	99.7
Global Avail [%]	42.1	45.2	49.6	59.7	75.9	86.9

Table S2. Keplerian vs. perturbed divergence over 720 hours.

Metric	Keplerian	Perturbed	Δ
N-ROI Avail [%]	87.66	89.05	+1.39
N-ROI GDOP	9.89	10.06	+0.17

Table S3. KLNS frozen-orbit element ranges over 720 h under the perturbed model.

Sat.	a_0 [km]	$\Delta a/a$ [%]	e_0	$e_{\max}$	i_0 [°]	Δi [°]
KLNS-1	12,000	0.59	0.70	0.776	70.0	3.24
KLNS-2	12,000	0.65	0.70	0.773	75.0	5.52
KLNS-3	12,000	0.60	0.70	0.775	75.0	4.26
KLNS-4	12,000	0.65	0.70	0.703	75.0	3.27
KLNS-5	12,000	0.57	0.70	0.778	68.0	5.06

Table S4. N-ROI availability at multiple GDOP thresholds (final 13-satellite constellation, 168 h, $\varepsilon_{\min} = 5^\circ$).

GDOP Threshold	N-ROI Avail [%]	Reduction vs. GDOP < 50
< 50	89.5	—
< 30	87.9	−1.6%p
< 20	82.0	−7.5%p
< 15	70.5	−19.0%p

Table S5. Elevation mask sensitivity (user-side masking re-evaluation; the $\varepsilon_{\min} = 5^\circ$ reference value does not coincide with the headline 89.5% of the Incremental Performance subsection owing to a discretisation difference between the two runs—the trend across mask values is the focus).

$\varepsilon_{\min}$	N-ROI NVS	N-ROI GDOP	N-ROI Avail [%]
5°	4.02	9.36	64.7
10°	3.71	11.30	53.8
15°	3.40	13.06	44.0

Table S6. PNT performance at KASA 2032 candidate landing sites (final 13-satellite constellation, 168 h, $\varepsilon_{\min} = 5^\circ$).

Site	Lat.	Lon.	NVS	GDOP	Base Avail [%]	KLNS Avail [%]
Gärtner	$+59.2^\circ$	$+34.6^\circ$	4.70	9.30	0.0	92.5
Endymion	$+53.6^\circ$	$+56.5^\circ$	4.69	10.32	0.0	94.2
Lacus Mortis	$+45.1^\circ$	$+27.2^\circ$	4.76	9.35	0.0	94.2
Clavius	-58.6°	-14.4°	6.59	6.48	99.8	100.0
Pingré	-58.6°	-73.7°	6.72	5.48	99.6	99.7
Maginus	-50.0°	-6.2°	6.27	7.17	99.9	100.0

Table S7. S-band link budget analysis (2491.8 MHz). The "Altitude" column reports the satellite altitude above the lunar surface at the indicated orbital phase, used here as a first-order proxy for slant range under the simplifying assumption of a sub-satellite user. A more thorough budget would account for off-nadir geometry and would yield a larger slant range (and FSPL) at the limb of the visibility footprint.

Scenario	Altitude [km]	FSPL [dB]	C/N_0 [dBHz]
Apolune (high)	18,663	185.8	32.2
Mid-range	9,158	179.6	38.4
Perilune (low)	1,863	165.7	52.3

Table S8. Stability pre-filter outcome.

Stage	Count
Total candidate orbits ($a \times e \times i \times \Omega \times M_0$)	10,368
After perilune filter ($r_p - R_{\text{Moon}} > 100$ km)	10,368
Removed by stability filter (Eqs. (2)–(5) of main text)	2,864
Final stable candidate pool	**7,504**